V International Conference on Particle-based Methods – Fundamentals and Applications
PARTICLES 2017
P. Wriggers, M. Bischoff, E. Oñate, D.R.J. Owen, & T. Zohdi (Eds)

TEXTURE AND STRESS TRANSMISSION IN BINARY GRANULAR COMPOSITES: COMPARISON BETWEEN SIMULATIONS AND EXISTING EXPERIMENTS

PAWARUT JONGCHANSITTO[1] AND ITTHICHAI PREECHAWUTTIPONG[1]

[1]Department of Mechanical Engineering, Faculty of Engineering, Chiang Mai University (CMU)
239 Huay Kaew Rd., Suthep, Muang district, Chiang Mai 50200, Thailand
e-mail: pawarut.j@cmu.ac.th and itthichai.p@cmu.ac.th

Key words: Molecular dynamics method, Granular media, Composites, Textures, Hydrostatic stresses.

Abstract. The morphology of two-dimensional cohesionless composite granular media obtained from thermoelastic stress analysis (TSA) experiments and molecular dynamics (MD) simulations is methodically compared by using the statistical analysis through the distributions of the hydrostatic stress in the particles and of the geometrical contact orientation between particles. Two different particles with a stiffness ratio of four between them are employed to prepare the numerical composite samples under study. Under a confined vertical compression in static conditions, experimental and numerical results are in good agreement in terms of the distributions of the hydrostatic stresses and of the contact directions.

1 INTRODUCTION

Sand, soil, and rock play a significant role in civil and geotechnical engineering to construct many infrastructures in our daily life, e.g. bridges, water dams, foundations, residential buildings, highways, etc. These are examples of granular materials, which are plentiful around us. In this context, a collection of solid particles, whose macroscopic mechanical behavior is governed by the inter-particle forces between contacts, is referred to as granular materials. They are composed from grains with a variety of sizes, shapes, and types of constitutive material. Due to a great diversity in grains, the behaviors of granular media are generally complex which cannot differentiate from those ordinary solids, liquids, and gases [1, 2]. Although this complexity remains far from well understood for researchers in many areas, there has been a significant effort for researchers describe and understand behaviors of granular materials during the past thirty years. Previous studies on granular mechanics mainly focus on mechanical behaviors of "non-composite" granular media, i.e. made of only one type of constitutive material, despite the fact that granular materials in engineering and industrial fields are prepared from various particles that their physical properties are different. That is why there is a lack of knowledge on mechanics of "composite" granular materials. Nonetheless, a few numerical and experimental studies pertaining to composite granular media can be found in the literature [3-6]. Recently, thermoelastic stress analysis (TSA) based on infrared (IR) thermography was experimentally performed to measure the hydrostatic stresses in the particles of two-dimensional composite

granular media [7]. This composite was prepared from two materials with different rigidity.

Since the first pioneering work performed more than the past four decades by Cundall ans Strack [8], the discrete or sometimes known as distinct element method (DEM) has proven to be a powerful and useful approach that provides a relationship between micromechanical data to macromechanical data by means of statistical mechanics [9]. The DEM was widely applied to investigate the mechanical behavior of non-composite granular media, e.g. the effects of the particle size and shape [10-12], the coefficient of friction [13], the surface energy [14] on contact force networks. From the authors' point of view, the DEM offers an effective way to investigate the mechanical behavior of composite granular materials. In this study, the molecular dynamics (MD) simulations which belong to the DEM are therefore applied to systematically model the two-dimensional non-cohesive composite granular system. Numerical results and experimental results obtained by thermoelastic stress analysis (TSA) experiments [7] are then statistically compared by using the granular texture in terms of distribution of the hydrostatic stress in the particles and contact orientation between particles. It must be noted that hydrostatic stresses provided by TSA experiments are used in this analysis instead of contact forces

The paper is organized as follows. Section 2 describes the theoretical aspects of MD simulations in terms of model for interaction forces, the details of numerical samples, and derivation of stress from contact forces. Section 3 is devoted to the statistical analysis and the comparison with experimental results.

2 THE MOLECULAR DYNAMICS MODELING

The molecular dynamics (MD) method relies on an explicit algorithm, which considers all particles of granular medium as rigid bodies with non-conforming surfaces [15]. The motions of each particle with respect to time are governed by Newton's equations of motion. These motion equations are numerically integrated using a predictor-corrector scheme with Gear's set of corrector coefficients [16].

2.1 Interaction force model

The interaction force model for contacting particles is an important part of the MD simulations. The interaction force is divided into a normal force and a tangential force. A variety of most commonly used force models in MD simulations was mentioned by Schäfer *et al.* [17]. In fact, local deformation in continuum mechanics occurs when two solid bodies are in contact [18]. Due to rigid bodies considered in the MD method, this deformation is easily modeled by using a virtual overlap δ at the contact point without change in the particle shape. The contact force is therefore calculated as a function of this virtual overlap (δ). In the case of circular disks, the virtual overlap between particles can be directly calculated from their vector position of the particle centers x_i and x_j and radii r_i and r_j:

$$\delta = \left(r_i - r_j\right) - \left|x_i - x_j\right| \tag{1}$$

In the case of $\delta > 0$, a simple model so-called the "linear spring-dashpot" [17-20] was employed to calculate the normal force between two particles in contact. The normal contact force can be separated into two components. The first component is an elastic repulsive force, which plays a role to withstand the deformation due to an external compression. It is simply

modeled as a linear spring. The second component is energy dissipation, which is relevant to an intrinsic characteristic of granular materials. It is represented through a viscous force. The expression of the normal force amplitude F_n can be written by

$$F_n = k_{eff}\delta + \alpha_n v_n \tag{2}$$

where k_{eff} is the effective contact stiffness, α_n is a normal damping coefficient, and v_n is the normal velocity (time derivative of the virtual overlap).

Due to the fact that the Coulomb's law of friction is a non-smooth function, we cannot directly apply this friction law to MD simulations. It can be additionally explained that the integration of Newton's equations of motion requires a smooth (mono-valued) friction law in such a way that the friction force can be mathematically expressed as a linear function of the sliding velocity v_s. As a consequence, the tangential force F_t in this study can be simply implemented by using a "regularized" form of the exact Coulomb's law [11, 17, 20], which can be computed by the following expression:

$$F_t = \min\left\{\left|\gamma_s v_s\right|, \mu F_n\right\} \cdot \mathrm{sign}\left(v_s\right) \tag{3}$$

where γ_s is the tangential viscosity coefficient and μ the coefficient of friction. It must be noted that the rotational motion due to the tangential force is allowed to be free in this study.

2.2 Preparation and simulation of numerical samples

Three similar composite configurations that used in the TSA experiments [7] were selected to prepare the two-dimensional numerical composite sample. This composite system was made of two constitutive materials with different rigidities as shown in Fig. 1a: polyoxymethylene (POM) appearing in black is termed a "stiff" particle, and high-density polyethylene (HDPE) appearing in white is a "soft" particle in the following. The stiff particle is approximately four times stiffer than the soft particle [7]. Table 1 gives the ratio of diameters D_{stiff}/D_{soft} and number of particles N_{stiff}/N_{soft} for each of the three configurations tested. Sample#1 is a monodisperse medium (D_{stiff}/D_{soft} = 1), whereas the others are bidisperse. It must be noted that in practice we aimed at analyzing only the effect of the D_{stiff}/D_{soft} ratio. This is a reason why the N_{stiff}/N_{soft} ratio for sample #1 and #2 are nearly close to 1, excluding sample #3. In addition, our analysis in the framework of 2D homogenization requires at least 300 particles to obtain relevant statistical values. This corresponds to the report in ref. [21] which mentioned that the linear scale of statistical homogeneity in a 2D assembly is a few tens of particle diameters. This criterion is reasonably satisfied for the three configurations under the study (see the last column in Table 1).

For each sample, the locations of particles were extracted from the optical image of real composite granular system from experiments (Fig. 1a). Such extracted positions were then employed to prepare the numerical samples inside a nearly square box consisting of four rigid plane walls. Fig. 1b presents an example of numerical preparation for sample #1. Under quasi-static conditions, a compressive vertical force of 60 kN was incrementally applied on the granular samples at the lower wall, while the other walls were still fixed during the test. The gravitational force was also considered during the simulations, even though it can be negligible compared to the magnitude of the external applied loading. It must be noted that all

contact types between particles consist of the contacts between stiff-stiff, soft-soft, and stiff-soft particles.

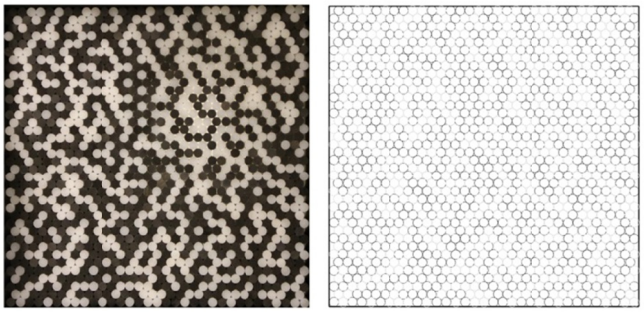

Figure 1: Experimental (a) and numerical (b) locations of the particles inside the composite sample #1.Note that for numerical sample, black color represents the stiff particle, while the soft one is indicated by grey color

Table 1: Three different samples used in this study

	Ratio of diameters D_{stiff} / D_{soft}	Number of cylinders N_{stiff} : N_{soft}	Ratio of cylinder numbers 1 : N_{stiff} : N_{soft}	Total number of cylinders
#1	1.0	638 : 597	1 : 0.94	1235
#2	1.6	334 : 371	1 : 1.11	705
#3	3.0	86 : 466	1 : 5.42	552

The normal and tangential forces between the inter-particle contacts are computed by using Eq. (2) and Eq. (3), respectively. The contact forces between wall and particles are also calculated by these expressions. Note that the effective contact stiffness k_{eff} is dependent of the types of contacting particles. The effective contact stiffness for the contact between stiff and soft particles is defined by $(k_{stiff} \times k_{soft})/(k_{stiff}+k_{soft})$. When the same types of material are in contact, k_{eff} is given by k_{stiff} for stiff and stiff contacting particles, by k_{soft} for soft and soft contacting particles. Furthermore, the contact stiffness in the case of the contact between wall and particles is simply considered by using the same value of k_{stiff}. The simulations were accomplished when the granular systems reached static equilibrium conditions. Next, the hydrostatic stress in each particle was determined from the list of normal and tangential forces obtained at the final stage of the simulations.

2.3 Determination of the hydrostatic stress in each particle

A definition of Cauchy stress tensor cannot be directly used in the meaning of granular (discrete) materials [22]. In addition, the simulations practically offer the forces between inter-particle contacts. In order to compare between the simulations and the experiments, it is necessary to derive the hydrostatic stress in each particle from the simulated interaction forces. In the past, several researches [23-25] proposed a stress tensor for discrete materials under equilibrium conditions, which relate the interaction forces in local scale to the stress tensor in macroscopic scale. The definition of the stress tensor at the macroscopic scale is

described by using a grain-by-grain approach based on the internal moment tensor $\mathbf{M}^{\mathbf{i}}$ of each particle p [25]. The symmetric second-order stress tensor σ_{ij} can be related to the interaction forces inside a granular assembly of volume V in the following way:

$$\sigma_{ij} = \frac{1}{V}\sum_{p\in V} M_{ij}^{p} = \frac{1}{V}\sum_{c\in V} f_i^c l_j^c \tag{4}$$

where the contact forces $f_1^c, f_2^c, \ldots, f_i^c$ act at the contact point c between the particles due to the external applied loading, and the vector l_j^c is the branch vector connecting the centroids of two particles in contact at point c. It is worth mentioning that the first summation in Eq. (4) is done over all particles, whereas the second summation is performed over the whole set of contacts within the volume V.

Next, the definition of the stress tensor at the macroscopic scale in Eq. (4) is developed at the particle scale to provide the stress tensor $\boldsymbol{\sigma}^{\mathbf{p}}$ in an individual particle. The stress tensor at the particle scale is calculated by the sum of the interaction forces and the radius vector of the particle at the contact point c along the particle perimeter over the particle volume V_p:

$$\sigma_{ij}^{p} = \frac{1}{V_p}\sum_{c\in V_p} f_i^c r_j^c \tag{5}$$

The list of normal and tangential forces obtained from the simulations is then employed to determine the stress tensor in each particle using Eq. (5). Under an assumption of plane stress satisfied in the present study, the eigenvalues of the stress tensor are used to compute the two in-plane principal stresses σ_1 and σ_2 of $\boldsymbol{\sigma}^{\mathbf{p}}$. The hydrostatic stress or average stress in each particle [24] is then determined by:

$$\sigma_{hyd} = \frac{(\sigma_1 + \sigma_2)}{2} \tag{6}$$

3 SIMULATION RESULTS AND COMPARISON WITH EXPERIMENTS

In this section, the numerical results obtained from MD simulations in this study and the experimental results obtained by thermoelastic stress analysis [7] are statistically analyzed by using the granular texture in terms of distribution of the hydrostatic stress in the particles and of the contact orientation between inter-particle contacts. Note that the results obtained by TSA experiments are fully described and discussed in a recent published paper (see ref. [7]).

3.1 Normalized hydrostatic stress networks

The simulations provide the network of normal contact forces for each sample as illustrated in Fig. 2a. The normal forces were represented by the red lines, whose thickness is proportional to the magnitude of the normal force. By comparing the three configurations, it is interesting to note that the larger particle size in granular system transmits the stronger force. Although the contact stiffnesses play a role in distribution of the force magnitude, the influence of polydispersity (in terms of particle size) on composite granular materials is still similar to what is observed in granular media made of only one type of constitutive

material [26]. Moreover, it is clearly observed that strong inhomogeneous interaction forces are exhibited in the composite system. This is a significant characteristic of non-composite granular medium. The normalized hydrostatic stress σ_{norm} networks for the simulations and experiments are shown in Figs. 2b and 2c, respectively. It must be noted that the definition of σ_{norm} is the ratio of the hydrostatic stress in the particle to the average hydrostatic stress value over the *whole* granular material. Similar to the contact force networks, heterogeneous stress fields are also observed in both monodisperse (sample #1) and bidisperse media (samples #2 and #3).

A triangular network, which mainly consists of straight lines inclined at ±60° with respect to the horizontal, is revealed in sample #1 for both the hydrostatic stress and contact force networks. This observation is not surprising due to the fact that the triangular network is a typical characteristic of monodisperse granular materials. It can be additionally seen that the highest stresses are found in the small particles for sample #2 and #3, although the strong force transmissions are provided by the larger particles as mentioned above. This can be explained by the fact that the division by V_p in Eq. (5) may cause high stress values when the particle size is small, even if this particle transmits low contact forces.

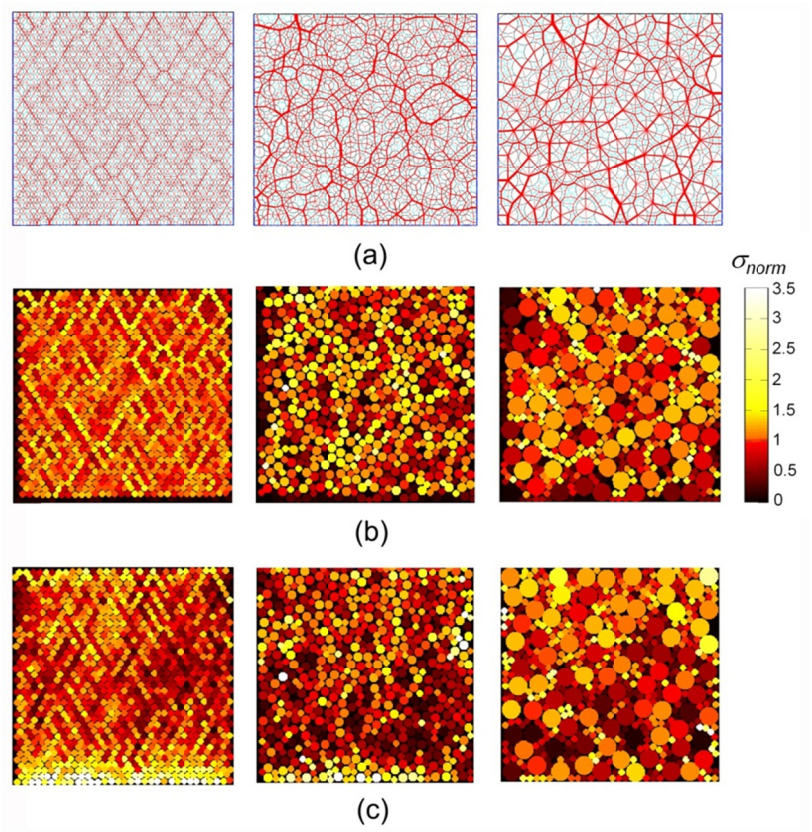

Figure 2: Results obtained for composite granular samples: (a) Normal contact force network obtained by MD simulation, (b) Field of normalized hydrostatic stress σ_{norm} determined from the simulated contact forces, and (c) Field of σ_{norm} obtained from the experiment

The differences between the hydrostatic stress networks obtained from simulations (Fig.

2b) and experiments (Fig. 2c) are anticipated. Indeed, it is not feasible to get precisely the same stress pattern between the experiment and the simulation at the particle scale. This may due to an inherent variation of parameters in any experiment: variation in terms of diameters, roundness, physical material properties, etc. A technical problem in the sense of particle locations may be also included. As a result, a micromechanical analysis of the experimental and numerical results is now performed through the granular texture.

3.2 Angular distribution of contact directions

In this section, the angular distribution of the contact directions is deduced from the experimental and numerical results. This is a useful statistical quantity to characterize the probability of contact orientation in each direction of the space. The angular distribution of the contact directions is relevant to the fabric tensor [27, 28], which enables us to understand the geometrical orientation of the particles and reveals a development of anisotropic structure of the granular system.

In the 2D representation, we characterize the angular distribution of contact directions by using the polar diagrams of the probability distribution $P(\theta)$ of the contact directions θ along the normal direction **n** as illustrated in Fig. 3. In this context, a definition of the function $P(\theta)$ is the ratio of the number of contacts in normal directions within an angular interval between $\theta - d\theta/2$ and $\theta + d\theta/2$ [28] to the total number of normal contacts in the system. There are 18 angular sectors lying between the angular range [0, 180°], which is plotted in the upper part of the diagram, while the bottom part corresponding to the range [0, -180°] is physically equivalent to the upper part. The contact between two particles in both the simulation and the experiment is detected when the distance between their centroids is lower than the sum of their radii. Four different types of contacts were analyzed by considering: all the contacts (Fig. 3a), only the stiff-stiff contacts (Fig. 3b), only the soft-soft contacts (Fig. 3c) and only the stiff-soft contacts (Fig. 3d). It must be noted that the term "all contacts" means all types of contact are considered: stiff-stiff, soft-soft, and stiff-soft. From Fig. 3, several comments can be made as follows:

- The contact directions in the monodisperse case (sample #1) are logically distributed along specific directions, i.e. 0°, 60°, and 120°, for whatever the type of contact considered: see the left column of Fig. 3. The polydisperse cases in samples #2 and #3 are taken into account. The contact directions are oriented in a quasi-homogeneous (isotropic) manner when the whole set of contacts are considered as shown in Fig. 3a. Considering the contact network between stiff-stiff particles in Fig. 3b, it can be clearly observed that the contacts are preferentially arranged along the axis of compression, i.e. the vertical axis, except for sample #3. In contrast, the other types of contact, i.e. soft-soft contacts in Fig. 3c and stiff-soft contacts in Fig. 3d, seem to be oriented along the specific directions as found in monodisperse case. These contact networks only play a role to maintain the granular system in equilibrium. In other words, the anisotropic structure of contacts between stiff-stiff particles is supported by such contact networks.
- The stiff-stiff contact network for sample #3 in Fig. 3b is considered. For both the experiment and the simulation, it is interesting to note that the distribution of the stiff-stiff contacts in sample #3 is inclined at about 45° from the vertical axis. This can be

explained by the fact relying on two reasons. First, a much difference between the cross-sections area of stiff particles and soft particles. Next, the effect of particle number on the contact orientations between soft and soft particles can be highlighted in sample #3 (Fig. 3c), which has a high number of soft particles compared to the number of stiff particles. The second reason leads to the contact directions between soft-soft particles tend to be arranged along particular directions as in the monodisperse case. Nevertheless, it can be noted that the contact network between stiff and stiff particles indeed makes an effort to arrange itself along the compression axis. As a consequence, the reason that is why the orientation of contacts between stiff-stiff particles in sample #3 is inclined at about 45° from the axis of compression is caused from a combination between the effect between stiff-stiff contact distributions and soft-soft contact distributions in this sample.

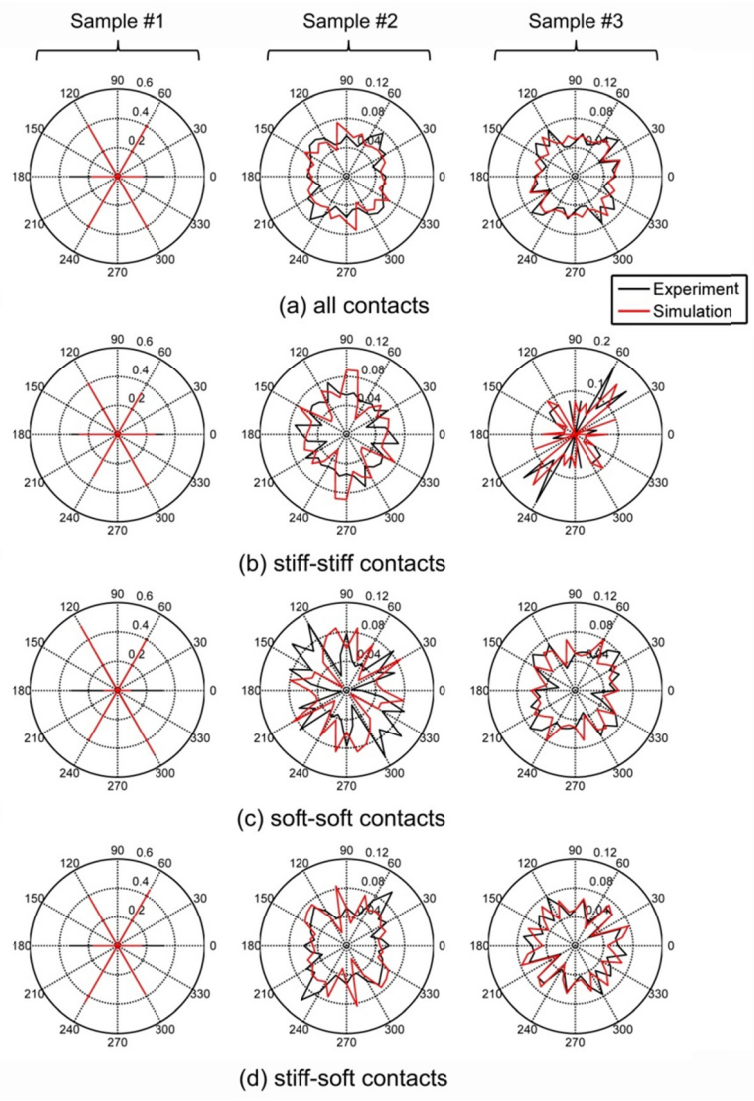

Figure 3: Polar diagram of the probability distribution of normal contact directions for each three composite samples: (a) all contacts, (b) only stiff-stiff contacts, (c) only soft-soft contacts, and (d) only stiff-soft contacts

From these several comments, it can be said that the results of the buildup of anisotropic structure owing to the mechanical loading obtained from the TSA experiments [7] and the MD simulations are good correlated from macroscopic point of view.

3.3 Statistical analysis of the hydrostatic stress distributions

In order to clearly characterize the distributions and correlations of the hydrostatic stresses in composite granular media, the probability distribution function P of the normalized hydrostatic stresses σ_{norm} for each sample is used in this section. As performed in the analysis of contact forces [29], we are able to separate the hydrostatic stress networks into two complementary networks by considering the average hydrostatic stress: the strong network and the weak network. The hydrostatic stresses which is greater than the average stress over the whole set of considered particles ($\sigma_{norm} \geq 1$) referred to as the "strong network", while the "weak network" consists of the particles carrying the hydrostatic stresses lower than the mean stress. The present work intends to analyze only the "strong network", because the high stresses are of great interest with regard to the breakage of granular materials in terms of particle crushing [30, 31]. The probability distribution functions of the normalized hydrostatic stresses in the strong network for each sample are plotted with normal scale (Fig. 4a) and with semi-logarithmic scale (Fig. 4b), respectively. Results provide three different analyses by considering only stiff particles, only soft particles, and then considering the whole set of the particles. It should be noticed that $P(\sigma_{norm})$ is determined by the ratio between the number of particles in the strong network and the total number of particles under the considered types of particle (stiff, soft, or both).

Let us now consider the whole set of the particles in Fig. 4, it is obvious that the functions $P(\sigma_{norm})$ are distributed as an exponential decay for both experiments and simulations. This distribution is characterized by the coefficient β, which can be written by the following expression:

$$P \propto e^{\beta(1-\sigma_{norm})} \tag{7}$$

This property corresponds to the well-known force distribution laws [20]. It is interesting to note that the exponential stress distribution law is also discovered in the strong network when only stiff particles and only soft particles are taken into account. In other words, the exponential distribution is a general characteristic of granular media in the strong network for both distributions of the contact force and the hydrostatic stress. This distribution shape is independent of the material types of the particle. Considering the value $P(\sigma_{norm} = 1)$ for all the particles in Fig. 4a, it is worth mentioning that the experimental and numerical percentages of particles in the strong network are mostly lower than 50%, i.e. $P(1) < 0.5$. This value is also observed for most of the experimental and numerical samples when only the stiff particles and only the soft particles are considered with respect to the total number of their own type. From these results in the sense of the stress distribution, it can be seen that both the experiments and the simulations are in good agreement.

Next, let us analyze the coefficient β in the semi-logarithmic plot as shown in Fig. 4b by means of the linear regression. This quantity can be used to compare the samples in terms of the probability to carry high stresses in the particles. There is high probability of a reaching significant hydrostatic stress in the granular media when the value of $|\beta|$ is low, while the

higher value of $|\beta|$ prevail to obstruct the particle crushing. For each of the three samples, the numerical values of $|\beta|$ are significantly lower than those of the experiments. It can be said that the probability to reach high stresses is overestimated by the simulations compared to the corresponding experiments. This situation is very useful if one uses simulations to design granular materials. However, the results follow the same trend between experiments and simulations: $|\beta_{\#1}| > |\beta_{\#2}| \approx |\beta_{\#3}|$. It can be observed that the two bidisperse composite samples exhibit a higher potentiality to carry high stresses than the monodisperse sample.

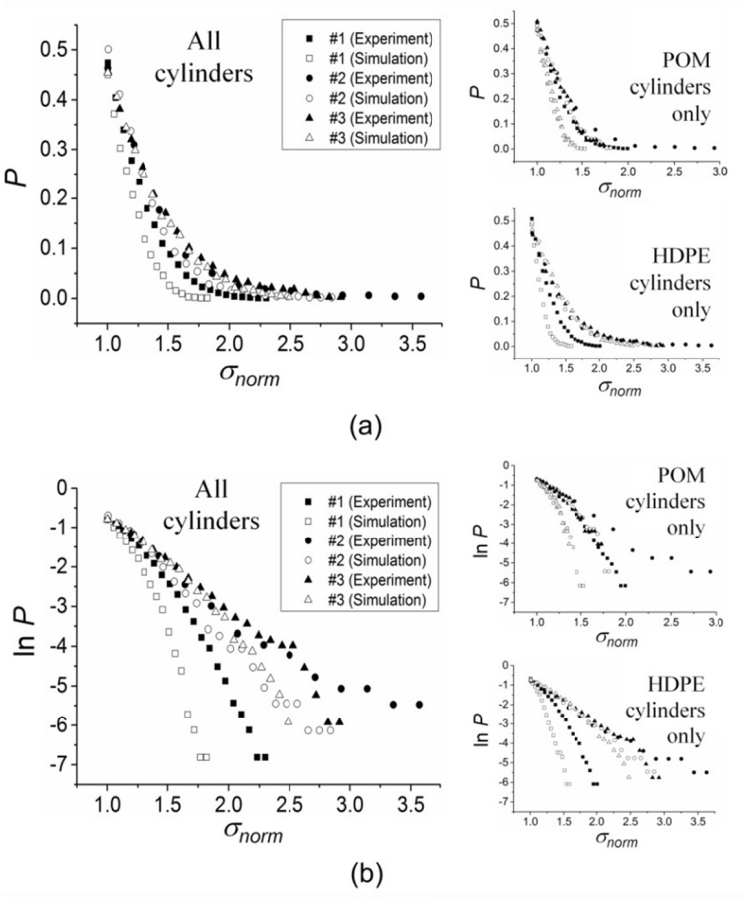

Figure 4: Probability distribution function P of the normalized hydrostatic stresses σ_{norm} in the strong network: plotting in (a) normal scale and (b) semi-logarithmic scale

4 CONCLUSION

The present study aimed at methodically analyzing the textural properties of 2D non-cohesive composite granular materials subjected to vertical confined compression. Molecular dynamics (MD) simulations were applied to model the three different composite configurations, which was completely tested by thermoelastic stress analysis (TSA) experiments [7]. The composite sample was constituted from two materials with different rigidities (stiff and soft particles). Both experimental and numerical results were compared in terms of hydrostatic stress distribution and contact direction distribution. It can be concluded that the experimental and numerical results follow the same trends in overview. In particular,

the distribution law of the hydrostatic stress in the strong network exhibits an exponential decay for all types of particle considered in the analysis (stiff, soft, or both), which is consistent with the well-known force distribution law [21]. In this network, there are less than 50% of particle numbers transmitting the stress greater than the average value. Considering in terms of geometrical orientation of the particles and their contacts in space, the anisotropic structure with an effort to arrange itself parallel to the direction of the external applied loading is evidently observed for the contact network between stiff and stiff particles. On the contrary, the equilibrium of the granular system is sustained by the other contact networks, i.e. soft-soft contacts and stiff-soft contacts.

Based on the global good agreement between experiments and simulations, it is important to notice that this study provides useful information obtained from the MD simulations in regard to composite granular materials. These numerical data are validated by the experimental data. In this manner, it can be said that the numerical simulations can be a supplementary tool to the experiments, in order to offer further information (difficult to obtain from the experiments) with regard to the mechanical behavior of composite granular media. Indeed, the optimum design of new composite granular systems could be done by using the simulations. Several parameters must be concerned in the design: constitutive material choice, proportion of particle number and size, and placement of particles in the system, for instance.

REFERENCES

[1] Jaeger, H.M. Sand, jams, and jets. *Phys. World* (2005) **18**(12):34-39.
[2] Jaeger, H.M. and Nagel, S.R. Granular solids, liquids, and gases. *Rev. Mod. Phys.* (1996) **68**(4):1259-1272.
[3] Budeshtskii, R.I. Mathematical model of granular composite materials. *Strength Mater+* (1971) **3**:912-916.
[4] Daraio, C., Nesterenko, V.F., Herbold, E.B., and Jin, S. Energy trapping and shock disintegration in a composite granular medium. *Phys. Rev. Lett.* (2006) **96**:058022.
[5] Wang, P.J., Xia, J.H., Li, Y.D., and Liu, C.S. Crossover in the power-law behavior of confined energy in a composite granular chain. *Phys. Rev. E* (2007) **76**:041305.
[6] Yang, Y., Wang, D., and Qin, Q. Quasi-static response of two-dimensional composite granular layers to a localized force. *Powder Technol.* (2014) **261**:272-278.
[7] Jongchansitto, P., Balandraud, X., Grédiac, M., Beitone, C., and Preechawuttipong, I. Using infrared thermography to study hydrostatic stress networks in granular materials. *Soft Matter* (2014) **10**(43):8603-8607.
[8] Cundall, P.A. and Strack, O.D.L. Discrete numerical-model for granular assemblies. *Géotechnique* (1979) **29**(1):47-65.
[9] Villard, P., Chavalier, B., Le Hello, B., and Combe, G. Coupling between finite and discrete element methods for the modeling of earth structures reinforced by geosynthetic. *Comput. Geotech*. (2009) **36**:709-717.
[10] Nguyen, D.H., Azéma, E., Radjai, F., and Sornay, P. Effect of size polydispersity versus particle shape in dense granular media. *Phys. Rev. E* (2014) **90**:012202.
[11] Peña, A.A., García-Rojo, R., and Herrmann, H.J. Influence of particle shape on sheared dense granular media. *Granul. Matter* (2007) **9**:279-291.
[12] Nouguier-Lehon, C., Cambou, B., and Vincens, E. Influence of particle shape and

angularity on the behaviour of granular materials: a numerical analysis. *Int. J. Numer. Anal. Meth. in Geomech.* (2003) **27**:1207-1226.
[13] Bardenhagen, S.G., Brackbill, J.U., and Sulsky, D. Numerical study of stress distribution in sheared granular material in two dimensions. *Phys. Rev. E* (2000) **62**(3):3882-3890.
[14] Preechawuttipong, I., Peyroux, R., Radjai, F., and Rangsri, W. Static states of cohesive granular media. *J. Mech. Sci. Technol.* (2007) **21**:1957-1963.
[15] Johnson, K.L. *Contact mechanics*. Cambridge University Press, (1985).
[16] Allen, M.P. and Tildesley, D.J. *Computer simulation of liquids*. Oxford Science Publications, (1987).
[17] Schäfer, J., Dippel, S., and Wolf, D.E. Force schemes in simulations of granular materials. *J. Phys. I* (1996) **6**:5-20.
[18] Matuttis, H.G., Luding, S., and Herrmann, H.J. Discrete element simulations of dense packings and heaps made of spherical and non-spherical particles. *Powder Technol.* (2000) **109**:278-292.
[19] Kruggel-Emden, H., Simsek, E., Rickelt, S., Wirtz, S., and Scherer, V. Review and extension of normal force models for the Discrete Element Method. *Powder Technol.* (2007) **171**:157-173.
[20] Jongchansitto, P., Preechawuttipong, I., Balandraud, X., and Grédiac, M. Numerical investigation of the influence of particle size and particle number ratios on texture and force transmission in binary granular composites. *Powder Technol.* (2017) **308**:324-333.
[21] Radjai, F., Jean, M., Moreau, J.J., and Roux, S. Force distributions in dense two-dimensional granular systems. *Phys. Rev. Lett.* (1996) **77**(2):274-277.
[22] Richefeu, V., Radjai, F., and El Youssoufi, M.S. Stress transmission in wet granular materials. *Eur. Phys. J. E* (2006) **21**:359-369.
[23] Kanatani, K. A theory of contact force distribution in granular materials. *Powder Technol.* (1981) **28**:167-172.
[24] Bagi, K. Stress and strain in granular assemblies. *Mech. Mater.* (1996) **22**:165-177.
[25] Cambou, B., Jean, M., and Radjai, F. *Micromechanics of granular materials*. John Wiley & Sons, (2009).
[26] Voivret, C., Radjai, F., Delenne, J.Y., and El Youssoufi, M.S. Multiscale force networks in highly polydisperse granular media. *Phys. Rev. Lett.* (2009) **102**:178001.
[27] Kruyt, N.P. Micromechanical study of fabric evolution in quasi-static deformation of granular materials. *Mech. Mater.* (2012) **44**:120-129.
[28] Rothenburg, L. and Bathurst, R.J. Analytical study of induced anisotropy in idealized granular materials. *Géotechnique* (1989) **39**:601-614.
[29] Radjai, F., Wolf, D.E., Jean, M., and Moreau, J.J., Bimodal character of stress transmission in granular packings. *Phys. Rev. Lett.* (1998) **80**(1):61-64.
[30] Russell, A.R., Wood, D.M., and Kikumoto, M. Crushing of particles in idealised granular assemblies. *J. Mech. Phys. Solids.* (2009) **57**:1293-1313.
[31] Arslan, H., Baykul, G., and Sture, S. Analysis of the influence of crushing on the behavior of granular materials under shear. *Granul. Matter* (2009) **11**:87-97.